30th NENE 2021
September 6 - 9
BLED-SLOVENIA
International Conference Nuclear Energy for New Europe

# Analytical Model of Debris Quenching with Top-Flooding Configuration and Additional Gas Injection for FLOAT Experiments

**Tim Kelhar[1], Markus Petroff[2], Janez Kokalj[1], Mitja Uršič[1], Rudi Kulenovic[2], Leon Cizelj[1], Jörg Starflinger[2]**

[1]Jožef Stefan Institute
Jamova cesta 39
SI-1000 Ljubljana, Slovenia
timy.kelhar@gmail.com, janez.kokalj@ijs.si, mitja.ursic@ijs.si, leon.cizelj@ijs.si

[2]Institute of Nuclear Technology and Energy Systems (IKE)
Pfaffenwaldring 31
D-70569, Stuttgart, Germany
markus.petroff@ike.uni-stuttgart.de, rudi.kulenovic@ike.uni-stuttgart.de,
joerg.starflinger@ike.uni-stuttgart.de

## ABSTRACT

A hypothetical severe accident in a nuclear power plant can result in the loss of reactor core integrity. In such case, the aim of severe accident management strategies is to achieve long-term stable conditions by having a coolable core geometry. Therefore, continuous analytical and experimental research is being performed in this field. Recently, a series of experiments at the FLOAT test facility of IKE, University of Stuttgart, Germany, were performed. The experiments were devoted to study the debris bed coolability for the case of top-flooding with water and the counter-current flow of gas injected at the bottom of the debris bed.

The paper presents past top-flooding experiments, recent FLOAT experiments and the description of the one-dimensional analytical model. The latter was used to enable preliminary assessment of experimental data from the FLOAT facility, i.e., to perform analyses of quenching behaviour. Obtained results demonstrated the ability of the analytical model to qualitatively describe the debris bed reflooding phase.

## 1 INTRODUCTION

One of the most important aspects of a nuclear facility is safety. The main safety concept for retention of radioactivity is defence-in-depth. If during an accident this concept fails, e.g., due to failure of multiple safety systems, the progression to a severe accident is possible. When part of the core is melted, it can be relocated to the lower head of the reactor vessel (RV), leading to a strong thermal stress on the RV internals (in-vessel scenario) [1]. If the RV fails, the melt is relocated to the reactor cavity, which can be wet or dry (ex-vessel scenario). In the cavity, the core melt will interact with the concrete underneath, which will generate non-condensable gases (NCG) at the bottom of the debris bed, flowing through the debris and altering the quenching process [1]. For severe accident management strategies, the coolability of the debris bed geometry in the RV or in the cavity is of utmost importance.

To simulate the debris bed quenching phase, we separate two main cases for the in-vessel or ex-vessel scenarios – the coolant (water) can either be injected from the bottom (bottom-flooding) or from the top (top-flooding). Quenching with different configurations was simulated with different test facilities and gives us an important inside look to the quenching process. For the ex-vessel scenario with a dry cavity, MCCI (molten core concrete interaction) is simulated by injecting NCG from the bottom. In most test facilities, the debris bed is simulated with small stainless-steel sphere-shaped particles, which are preheated to simulate the heat-generating debris bed. When simulating MCCI with additional gas injection, depending on the flooding configuration, the counter-current flow can develop and usually gas (and generated steam) acts against penetrating water and hinders its flowing paths. This lowers the ability to cool the debris bed and in the most cases extends the quenching process [1].

In the past, several experiments have been performed. In experiments of Tung et al. [2], the main focus was on the effect of additional gas injection on the coolability of the debris bed. The substitute for the debris bed were stainless-steel particles with diameter of 1.6 mm. It was shown that a simulation of NCG can cause a premature halt of quench progression, what consequently lowers the cooling capabilities [1]. In the DEBRIS facility at IKE, University of Stuttgart, Germany, experiments with top-flooding and bottom-flooding cooling configuration can be performed [3]. The bed in the DEBRIS facility is heated volumetrically. The main test section consists of a ceramic crucible with a total height of 870 mm and an inner diameter of 150 mm. The top-flooding experiments showed that after a short time, water starts to penetrate downwards into the bed preferably faster near the wall regions than in the rest of the bed until it reaches the bottom. This is caused by lower debris bed temperature and higher porosity near the wall (wall effect) [3]. Once the water reaches the bottom of the debris bed, the quenching front upward progression could be approximated to be one-dimensional [3].

For ongoing experiments, a new FLOAT test facility (IKE) was built. The main addition to the quenching experiments performed on DEBRIS is the possibility for bottom gas injection, in order to simulate MCCI. A total of 9 top-flooding experiments were already presented by Petroff et al. [1]. In the experiments, two main parameters were varied – initial debris bed temperatures and the injection of NCG through the debris bed. The maximal bed temperatures were 300°C or 500°C; gas flow injection with a flow rate of 140 l/min was used in four of the tests. The results showed that a higher initial temperature of stainless-steel spheres and presence of NCG prolongs the quenching time.

The purpose of our research is to perform analytical analyses of the FLOAT experiments. The first objective is to analyse selected FLOAT experiments to extract data for further analytical investigation. The second objective is to develop a simplified analytical model, capable to calculate the amount of water involved in the reflooding phase.

## 2 FLOAT EXPERIMENTS

### 2.1 Description of the test facility

The FLOAT test facility was developed at IKE for conducting specific reflooding experiments with additional gas injection [1]. It features configurations for performing bottom flooding (Figure 1(A)) and top flooding (Figure 1(B)) experiments. The FLOAT test facility has a wider bed diameter of 200 mm and shorter bed height of 300 mm, compared to the DEBRIS test facility [1]. The FLOAT has an installed water flow meter (Figure 1(D)). In case of top-flooding configuration, water is uniformly distributed over the debris bed area by a spray head, located above the test section (Figure 1(B)). At the top of the test section, the steam mass flow meter is installed (Figure 1 (C)). The debris bed (Figure 1(E)) is composed of pre-oxidised stainless-steel sphere-shaped particles with diameter of 6 mm. The debris bed is volumetrically heated by a water-cooled induction coil (Figure 1(F)), connected to a radio frequency generator,

generating maximal output power of 40 kW. The quartz glass test section is equipped with 45 shielded thermocouples laterally arranged at 3 different radial positions – most of the thermocouples are located near the wall (R=90 mm), the rest of the sensors are disposed in the centre (R=0 mm) and at half radius (R=50 mm) positions. The main addition of the FLOAT facility, compared to the DEBRIS facility, is the injection of NCG (Figure 1 (G)) that is preheated (Figure 1 (H)). For the NCG, air is used. Air is led to four perforated pipes where it is homogenously injected through the ceramic particle layer (Figure 1 (I)) into the debris bed cross-section. The test section is laterally well insulated to minimize the thermal losses [1].

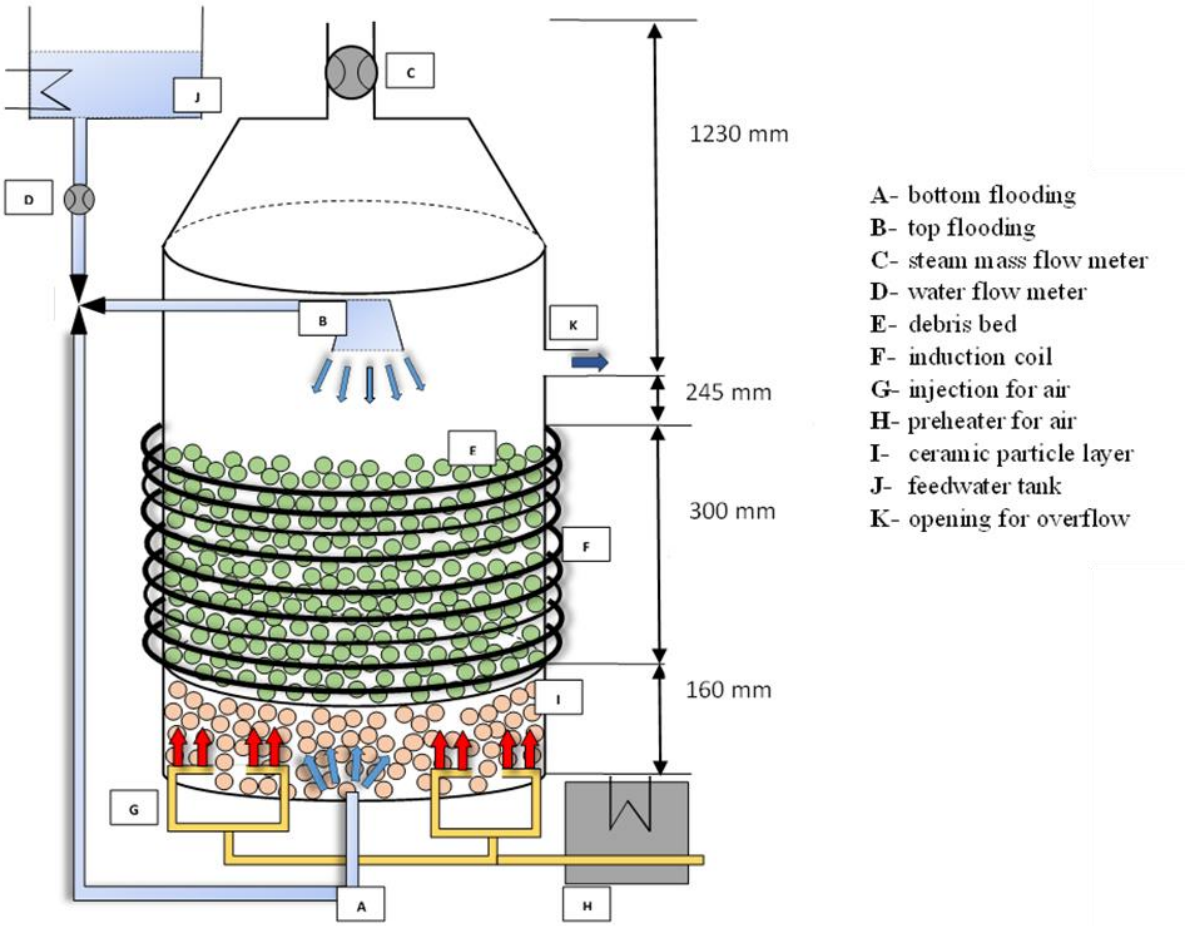


Figure 1: Scheme of the experimental test facility FLOAT with different flooding configurations. Dimensions are taken from [1].

## 2.2 Initial conditions

In all experiments summarized in Table 1, the debris bed was initially preheated by inductive heating. Experiments were conducted at ambient conditions. For experiments with additional air flow, the volume flow control unit was activated to homogenously inject preheated air at a rate of 140 l/min at different temperatures into the bottom of the test section [1]. Immediately after the start of the air flow injection, the water injection was initiated to start the quenching process. The experiments were finished when all the thermocouples were cooled down at the water saturation temperature of 100°C [1]. A total of four top-flooding experiments with maximal initial debris bed temperatures of 500°C and 700°C are analysed. Experiments at each temperature were performed under two different conditions, with and without the air injection.

Table 1: Initial conditions and results obtained from experimental data.

| Experiment | | F.6 | F.14 | F.32 | F.33 |
|---|---|---|---|---|---|
| **Debris bed** | Mass [kg] | 44.17 | 44.22 | 44.17 | 44.11 |
| | Porosity [-] | 0.40 | 0.41 | 0.41 | 0.41 |
| | Initial temperature [°C] | 500 | 500 | 700 | 700 |
| **Water** | Flow [l/min] | 6.8 | 6.5 | 4.7 | 4.3 |
| | Initial temperature [°C] | 67 | 85 | 80 | 82 |
| **Air** | Flow [l/min] | 140 | / | 140 | / |
| | Initial temperature, $T^0_{air}$ [°C] | 97 | | 81 | |
| **Results** | Duration of stage 1 [s] | 36 | 42 | 125 | 131 |
| | Duration of stage 2 [s] | 157 | 88 | 128 | 110 |

## 2.3 Experimental results with discussion

As seen in Table 1 and Figure 2, experiments with the top-flooding configuration can be divided into two stages:

- Stage 1 is defined as the period from the start of top-flooding until the moment when the bottom of the debris bed is considered to be completely flooded. We can see how in the conducted experiments, F.6 and F.14, water mainly penetrates downwards at the near-wall regions, until it reaches the bottom of the bed. Tests with a higher maximal initial debris bed temperature, i.e. F.32 and F.33, have shown a shift of the initial quenching path from the wall region to the inner region. This shift might be attributed to the presence of limescale at the spray head, resulting also in a lower water injection rate (see Table 1).
- Stage 2 is defined as the period until the remaining part of the superheated debris bed is quenched by the elevation of water level and by the local accumulating water pools [1]. As seen in Figure 2, not all thermocouples are quenched at the same elevation level at the same time. When only one thermocouple at a high elevation level is quenched, this could be due to the local penetration of water from the wall regions towards the inner regions, or could be due to the water penetrating downwards locally and quenching only one thermocouple.

From Figure 2, we can observe that times of the first thermocouple being quenched at the bottom are more or less the same for experiments with the same maximal initial bed temperatures. However, as indicated in Figure 2 and summarized in Table 1, the start (quenching front at position 0 mm) and duration (quenching front at position 300 mm) of stage 2 was defined by linear fitting of the experimental data. Test F.14 was performed without additional air flow and resulted in initial 42 s of quenching time for stage 1 and final 88 s for stage 2, while test F.6 with additional air flow resulted in a duration of stage 1 of 36 s and had an extended quenching time of 157 s for stage 2. The same results can be obtained from the F.33 and F.32 experiments, when latter had an extended quenching time of stage 2 for 18 s, comparing to F.33. These results show the importance of NCG generated during MCCI on the inhibition of debris bed reflooding.

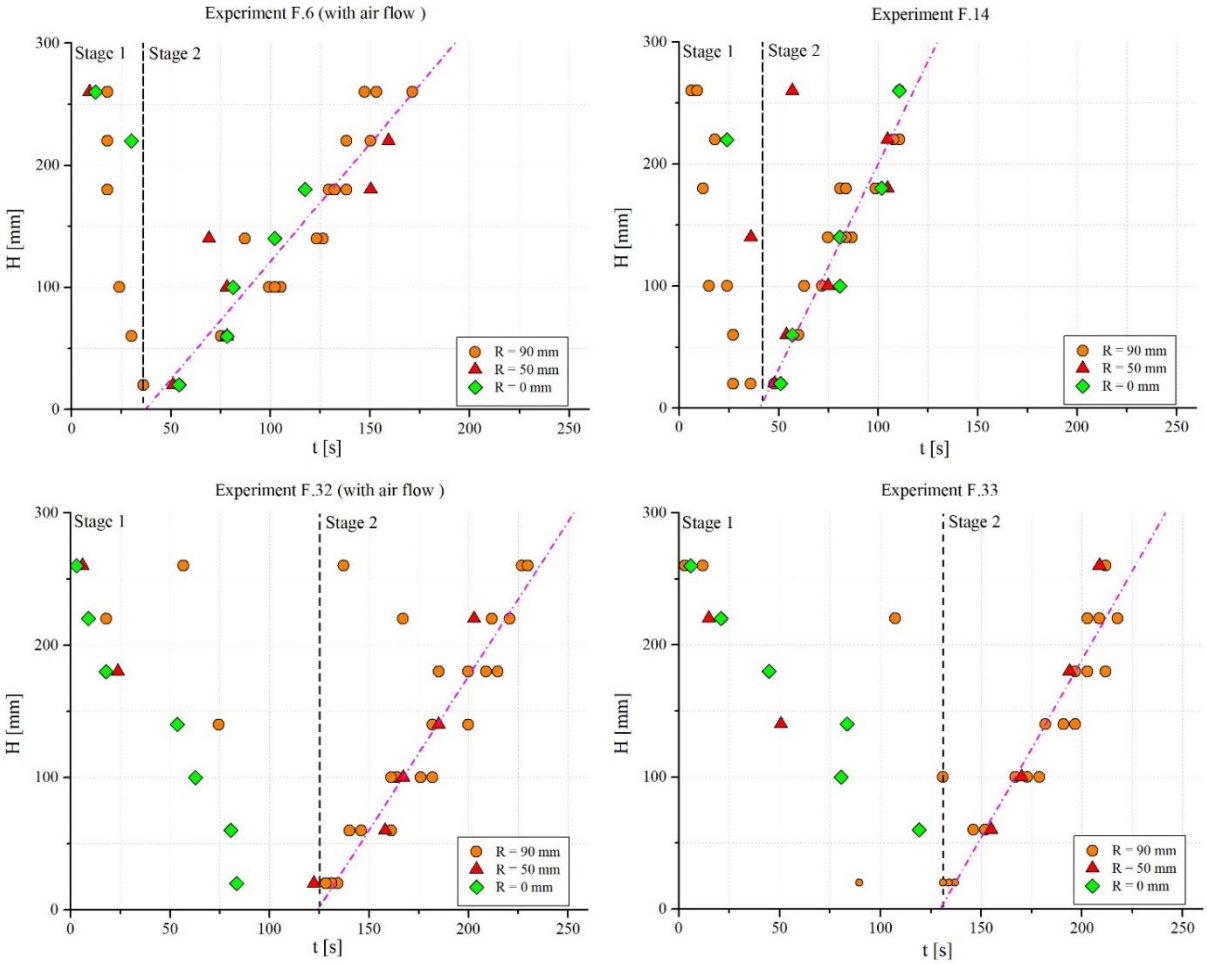


Figure 2: Experimental results of quenching front propagation for 4 top-flooding FLOAT experiments (see Table 1). Symbols represent quenched thermocouples at different elevation levels and radial positions. Dashed-purple line is a linear fit of the experimental data.

## 3 ANALYTICAL MODEL

To make a preliminary assessment of the experimental data, a simple one-dimensional analytical model was developed. Our analytical model follows the approach made by Tutu et al. [6], [7] and Kokalj [5]. The approach is applicable for the description of the debris bed quenching during the reflooding stage, i.e. stage 2 of the FLOAT experiments.

### 3.1 Model description

As Figure 3 suggests, the analytical model differentiates 2 volume regions: bottom part filled with injected water and air, and upper part that contains a mixture of steam and air. Full volume is filled with debris particles with volume fraction $1-\varepsilon$, where $\varepsilon$ refers to porosity. Our main assumptions for the analytical model are:

a. Water is entering beneath the bottom part with constant velocity $u_l^0$ and temperature $T_l^0$.
b. Quenching front is shifting upwards with velocity $U_q$ and coincides with the water level.
c. Phase change and the heat transfer instantaneously occur at the quenching front. Stainless steel is quenched from the initial temperature $T_{SS}^0$ to the water temperature $T_l^0$.
d. On the top of the upper volume, steam is exiting with the temperature of stainless-steel particles, $T_{SS}^0$, and with velocity $u_g$.

e. Air (if used), enters at the bottom with constant velocity $u_{air}^0$ and at temperature $T_{air}^0$. At the exit, its velocity is $u_g$ and has the temperature $T_{SS}^0$. The change of the gas temperature occurs at the quenching front.

Assumption *a* is valid, as stage 1 cannot be simulated with the proposed analytical model. For example, the one-dimensional model cannot consider possible counter current flows and areas where water is not penetrating homogenously. Thus, with our model it is presumed that flooding starts at the beginning of stage 2 – when the full bottom of the bed has been quenched. For that reason, the experimental data at the initiation of stage 2 have to be considered as initial conditions.

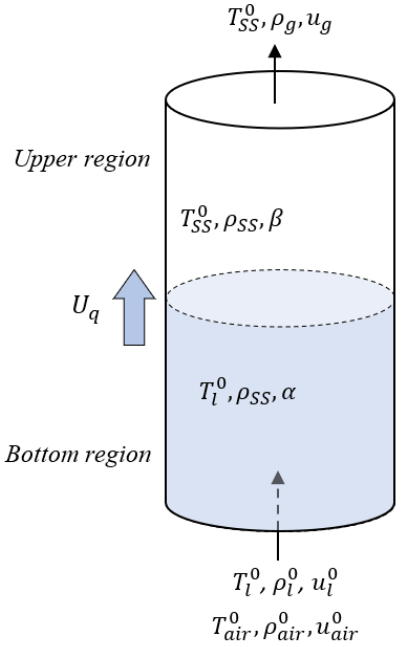


Figure 3: Schematic display of bottom flooding configuration with initial and boundary conditions.

## 3.2 Balance equations

The mass balance equation for the presented model is:

$$\rho_l^0 u_l^0 + \rho_{air}^0 u_{air}^0 - \rho_g u_g = U_q \varepsilon \left[(1-\alpha)\rho_l^0 + \alpha \rho_{air}^0 - \rho_g\right], \tag{1}$$

where index *l* refers to water, *g* is for mixture of steam and air (if used) and $\rho$ represents density. The left side of Eq. (1) represents the injected water and air, and the discharged mixture of steam and air. The expression on the right-hand side is for change in accumulated water, air and mixture inside the considered domain. Parameter α is the volume fraction of air in the bottom area. In our model, its determination is done by equalizing the pressure drop for air and water in a porous media by considering semi-empirical equation [8]:

$$\frac{\rho_l^0}{\mu\mu_l}(u_l^0)^2 + \frac{\eta_l}{\kappa\kappa_l} u_l^0 + \rho_l^0 g = \frac{\rho_{air}^0}{\mu\mu_{air}}(u_{air}^0)^2 + \frac{\eta_{air}}{\kappa\kappa_{air}} u_{air}^0 + \rho_{air}^0 g, \tag{2}$$

where superficial velocities $(u_i^0)$, dynamic viscosities $(\eta_i)$, relative passabilities $(\mu_i)$, and relative permeabilities $(\kappa_i)$ are properties for air $(air)$ and water $(l)$. The relative passability and the relative permeability of the water and air are defined by applying the Lipinski-Reed model parameters for a two-phase flow [8] (i.e. determination depends on parameter $\alpha$). The

passability (μ, in units of m) and permeability (κ, in units of $m^2$) of the debris bed are defined by applying the Ergun equation (i.e. determination depends on the porosity and debris bed particles size) [8].

The internal energy balance equation for the presented model is:

$$\rho_l^0 u_l^0 h_l(T_l^0) + \rho_{air}^0 u_{air}^0 h_{air}(T_{air}^0) - \rho_g u_g h_g(T_{SS}^0) = \\ = U_q(1-\varepsilon)\rho_{SS}\left(h_{SS}(T_l^0) - h_{SS}(T_{SS}^0)\right) + U_q\varepsilon(1-\alpha)\rho_l^0 h_l(T_l^0) + U_q\varepsilon\alpha\rho_{air}^0 h_{air}(T_{air}^0) - U_q\varepsilon\rho_g h_g(T_{SS}^0), \quad (3)$$

where $h(T)$ is enthalpy at temperature *T*. Index *SS* refers to stainless steel (i.e. debris bed). On the left-hand side of Eq. (3), the three parts represent the difference between internal energies of inlet water and air, and outgoing mixture. The debris bed particles in the upper area are only in contact with the mixture, and have the temperature $T_{SS}^0$, while in the lower area they are cooled down to the water inlet temperature $T_l^0$ (the first part on the right-hand side of Eq. (3)). The second, third and fourth part on the right-hand side of Eq. (3) represent the changes of internal energy in the considered domain for the water, air and gas mixture, due to the motion of the quenching front.

Finally, the conditions of the gas mixture have to be defined for Eqs. (1) and (3). Density and enthalpy of the discharged mixture are calculated by the following equations:

$$\rho_g = \beta \cdot \rho_{air} + (1-\beta)\rho_{steam}, \quad (4)$$

$$\rho_g h_g(T_{SS}^0) = \beta \cdot \rho_{air} h_{air}(T_{ss}^0) + (1-\beta)\rho_{steam} h_{steam}(T_{SS}^0). \quad (5)$$

It is assumed that both components of mixture (i.e. air and steam) at the exit of the upper region are coupled and have the same temperature ($T_{SS}^0$) and velocity ($u_g$). Parameter $\beta$ is determined by equalizing the inlet and outlet air mass flow:

$$\beta = \frac{\rho_{air}^0 u_{air}^0}{\rho_{air} u_g}. \quad (6)$$

## 4 CALCULATIONS WITH ANALYTICAL MODEL

Here, our primary objective is to estimate the water flow involved in the stage 2 with the usage of the analytical model presented in Section 3. Namely, during the FLOAT experiments the overflow of water entering from the spray head (see Figure 2) was observed and thus, not all water flow given in Table 1 could be considered to contribute to the quenching process during the stage 2.

From the Eqs. (1) and (3), the volume flow rate of injected water for the stage 2 can be calculated,

$$u_l^0 A = \\ \frac{U_q A\left(\varepsilon\left[(1-\alpha)\rho_l^0\left(h_l(T_l^0) - h_g(T_{SS}^0)\right) + \alpha\rho_{air}^0\left(h_{air}(T_{air}^0) - h_g(T_{SS}^0)\right)\right] + (1-\varepsilon)\rho_{SS}\left(h_{SS}(T_l^0) - h_{SS}(T_{SS}^0)\right)\right) - \rho_{air}^0 u_{air}^0\left(h_{air}(T_{air}^0) - h_g(T_{SS}^0)\right)}{\rho_l^0\left(h_l(T_l^0) - h_g(T_{SS}^0)\right)}, \quad (7)$$

where *A* is the surface area of the FLOAT test section. In Eq. (2), the parameter $\alpha$ is a function of $u_l^0$ and must thus be defined iteratively. Also, parameter $\beta$ defined with Eq. (6) must be calculated iteratively, as $u_g$ is implicitly a function of $\beta$ being defined from Eq. (1).

### 4.1 Determination of initial and boundary conditions

Quantities for Eq. (7) are summarized in Table 2 and elaborated hereafter.

Table 2: Initial conditions for analytical model with results.

| Experiment | | F.6 | F.14 | F.32 | F.33 |
|---|---|---|---|---|---|
| **Ambient condition** | p *[bar]* | 1.0133 | | | |
| **Quenching front** | $U_q$ *[mm/s]* | 1.9 | 3.4 | 2.3 | 2.7 |
| **Debris bed** | $\rho_{ss}$ *[kg/m³]* | 7811 | 7952 | 7943 | 7932 |
| | $\varepsilon$ *[-]* | 0.4 | 0.41 | 0.4 | 0.41 |
| | $T_{ss}^0$ *[°C]* | 346 | 300 | 269 | 199 |
| | $h_{ss}(T_l^0)$ *[kJ/kg]* | 187 | | | |
| | $h_{ss}(T_{ss})$ *[kJ/kg]* | 310 | 287 | 271 | 236 |
| **Water** | $\rho_l^0$ *[kg/m³]* | 958 | | | |
| | $T_l^0$ *[°C]* | 100 | | | |
| | $h_l(T_l^0)$ *[kJ/kg]* | 419 | | | |
| | $\eta_l$*[μPa s]* | 282 | / | 282 | / |
| **Steam** | $\rho_{steam}(T_{ss}^0)$ *[kg/m³]* | 0.355 | 0.384 | 0.406 | 0.467 |
| | $h_{steam}(T_{ss}^0)$ *[kJ/kg]* | 3168 | 3075 | 3012 | 2873 |
| **Air** | $\rho_{air}^0$ $(T_{air}^0)$ *[kg/m³]* | 0.954 | / | 0.997 | / |
| | $\rho_{air}$ $(T_{ss}^0)$ *[kg/m³]* | 0.570 | | 0.652 | |
| | $T_{air}^0$ *[°C]* | 97 | | 81 | |
| | $h_{air}(T_{air}^0)$ *[kJ/kg]* | 372 | | 356 | |
| | $h_{air}(T_{ss}^0)$ *[kJ/kg]* | 622 | | 545 | |
| | $\eta_{air}$ *[μPa s]* | 22 | | 21 | |
| | $u_{air}^0$*[m/s]* | 0.074 | | 0.074 | |
| **Calculated parameters** | $\alpha$ *[-]* | 0.28 | / | 0.28 | / |
| | $\beta$ *[-]* | 0.10 | | 0.12 | |
| **Results** | $u_l^0 A$ *[l/min]* | 1.8 | 3.8 | 2.0 | 2.6 |

For the quenching front velocity, the experimental values obtained from Figure 2 are used. Consequently, the applied duration of reflooding in the calculations are the same as duration of the stage 2 in the experiments (see Table 1).

To keep the experimental data on the particle mass (see Table 1), the density of the debris bed is calculated via mass of the debris bed, porosity and volume of the FLOAT test facility. The debris bed consists of 6 mm pre-oxidised stainless-steel spheres. At the beginning of stage 2, the temperature of bed particles has importantly changed compared to the initial temperature, due to the quenching at the wall regions (experiments F.6 and F.14) or central regions (experiments F.32 and F.33) during the stage 1. Thus, the initial temperature of particle debris

bed at the beginning of stage 2 was defined as an average of volumetrically weighted temperature of all thermocouples. For defining the volumetric weight, the debris bed was divided into 3 segments on every height with radius 0 mm to 25 mm, 25 mm to 75 mm and 75 mm to 100 mm. Depending on the position of every thermocouple in each segment, their weighting factor was calculated. The final debris bed particle temperature is set to the water saturation temperature. For the calculation of the enthalpy the specific heat of 500 J/kg/K is considered.

The properties of water and steam are defined using the tables. The properties for air were calculated assuming air being an ideal gas. Initial temperature of water was set to the saturation temperature. Indeed, near saturation temperatures are expected because of the water heating during its penetration from the spray to the bottom region and because of mixing in the ceramic particle layer (see Figure 1). The initial temperature of air is set to the experimental value. The final temperature of steam and air are set to the initial temperature of the particle debris bed.

### 4.2 Results with discussion

The estimation of the water flow involved in the stage 2 is presented in Table 2. The air flow inhibits the water flow, and if considering the duration of stage 2, also the total amount of water used to quench the debris bed. Comparing our calculation results with the experimental results in Table 1, we can estimate that both cases, that were conducted without air injection used around 60% of initial water entering the test section from the spray. On the other hand, F.6 used approximately 26% of water and F.32 used approximately 42% of water compared to the experimental data.

By calculating the mass flow of the discharging mixture with Eq. (1), we can support our analytical model, as we can compare analytical results with experiments (see Figure 4). Due to troubles of measuring mass flow rate for experiments F.6 and F.14, only results from experiments with initial temperatures of 700°C are presented in Figure 4. In the figure, the integrated discharged mass is higher in the calculation cases compared to the experimental data. The reason for that might be in the condensation of discharged steam that could not be completely prevented in the experiments due to the presence of local subcooled surfaces resulting from inhomogeneities in the debris bed particle heating and quenching. Also, in the experiment the subcooled water pool above the debris bed is causing condensation of the through-flowing steam. Case F.33, without air injection, shows better agreement with the experimental data, than F.32. The reason for mismatch could be due to analytical model not considering the NCG precisely enough. Nevertheless, it shows that our model is accurate enough for qualitative assessment.

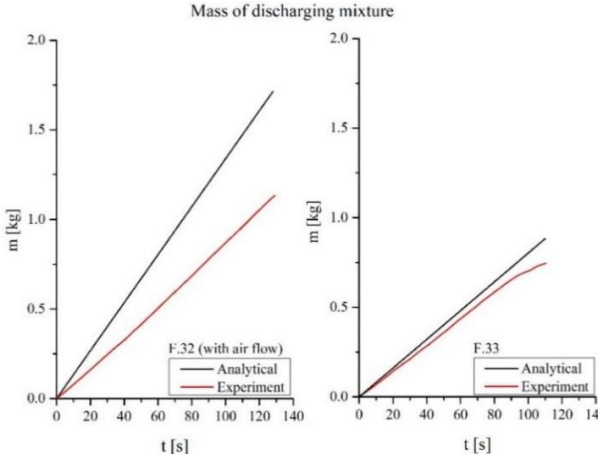


Figure 4: Comparison of analytical model and experimental results for mass flow of discharging gas.

To obtain more accurate results, the experiments shall be modelled in more details. For example, the real effect of gas flow on the quenching front propagation could be estimated by considering the momentum balance equation and inhibiting effect of the gas presence on the heat transfer between the debris bed and water. This is possible with the computational fluid dynamic codes having capabilities to consider 2-D or 3-D effects, e.g., ATHLET (GRS, Germany) or MC3D (IRSN, France). The capability of MC3D for this kind of experiments has been already demonstrated for simulation of the bottom flooding experiment PEARL (IRSN, France) [4], and for the top flooding experiments [9].

## 5 CONCLUSIONS

The simplified one-dimensional analytical model enables the qualitative description of the debris bed reflooding. The disadvantage of the analytical model is that it cannot describe all the transient activities during the water penetrating downwards and then reflooding. Thus, the future aim at JSI is to simulate these experiments with the MC3D code (IRSN, France), which considers 2-D and 3-D effects, and will consequently provide insights in the quenching behaviour, enabling us to assess the impact of NCG and the top-flooding on quenching of hot particle debris bed in the FLOAT facility.

## ACKNOWLEDGMENTS

The authors acknowledge the financial support of the Slovenian Research Agency within the research program Reactor engineering (P2- 0026) for the work performed at the Jožef Stefan Institute (JSI). The JSI authors acknowledge the University of Stuttgart, Institute of Nuclear Technology and Energy Systems (IKE) who have developed original FLOAT experimental data. Results of FLOAT experiments are available at Jožef Stefan Institute within the written agreement.

## REFERENCES

[1] M. Petroff, R. Kulenovic, J. Starflinger, Experimental Investigation on Debris Bed Quenching with Additional Non-Condensable Gas Injection, 29th International Conference Nuclear Energy for New Europe, September 2020, Portorož, Slovenia.

[2] V.X. Tung, V.K. Dhir, D. Squarer, Quenching by top flooding of a heat generating particulate bed with gas injection at the bottom, Sixth information exchange meeting on debris coolability: proceedings, EPRI-NP-4455, 1986.

[3] M. Rashid, S. Rahman, R. Kulenovic, M. Bürger, E. Laurien, Quenching Experiments: Coolability of Debris Bed, Nuclear Technology, Volume 181(1), 2013, pp. 208-215.

[4] J. Kokalj, M. Uršič, M. Leskovar, L. Piar, R. Meignen, Modelling of debris bed reflooding in PEARL experimental facility with MC3D code, Nuclear Engineering and Design, Volume 330, 2018, pp. 450-462.

[5] J. Kokalj, Modeliranje poplavljanja plasti razbitkov v eksperimentalni napravi PEARL, Master's Thesis, University of Ljubljana, 2016.

[6] N.K. Tutu, T. Ginsberg, J. Klein, C.E. Schwarz, J. Klages, Transient quenching of superheated debris beds during bottom reflood, BNL-NUREG 35287, 1984.

[7] N.K. Tutu, T. Ginsberg, J. Klein, C.E. Schwarz, J. Klages, Debris bed quenching under bottom flood conditions (in-vessel degraded core cooling phenomenology), NUREG/CR 3850, 1984.

[8] L. Li, K. Wang, S. Zhang, X. Lei, An experimental study on two-phase flow resistances and interfacial drag in packed porous beds, Nuclear Engineering and Technology, Volume 50, Issue 6, 2018.

[9] A. Larrauri, R. Meignen, M. Gradeck, N. Rimbert, Analytical Transient Two-Phase Model For Dry-Superheated Debris Bed Under Top Flooding Conditions, NURETH 18 conference, August 2019, Portland (Oregon), United States.